

Received March 7, 2022, accepted March 28, 2022, date of publication March 30, 2022, date of current version April 8, 2022.

Digital Object Identifier 10.1109/ACCESS.2022.3163448

# Comparison of AC and DC Partial Discharge by Monitoring of Vacuum Degree in a Distribution Class Vacuum Interrupter

SEUNGMIN BANG<sup>ID</sup>, HYUN-WOO LEE, AND BANG-WOOK LEE<sup>ID</sup>, (Senior Member, IEEE)

Department of Electrical Engineering, Hanyang University, Ansan 15588, South Korea

Corresponding author: Bang-Wook Lee (bangwook@hanyang.ac.kr)

This work was supported by the National Research Foundation of Korea (NRF) Grant through the Republic of Korea Government [Ministry of Science and ICT (MSIT)] under Grant 2021R1F1A104554711.

**ABSTRACT** The vacuum degree of Vacuum Interrupter (*VI*) will deteriorate because of gases emitted by arc heat, and leakage through the joints. It is important to select an appropriate maintenance criteria for a *VI* by monitoring the vacuum degree. However, monitoring of a *VI* installed inside a solid insulation apparatus in a transmission system is impossible. Only studies on the insulation deterioration because of the decrease of the vacuum degree have been conducted, and important factors such as the maintenance criteria have not been investigated. Moreover, most studies have only been performed using AC voltage, not DC voltage. Therefore, in this paper, AC and DC partial discharge were compared by monitoring of the vacuum degree in a distribution class *VI* to propose maintenance criteria according to voltage type. Through this, for efficient maintenance, maintenance criteria of *VI* for each voltage type are presented. The vacuum degree at which the dielectric strength rapidly decreases was confirmed according to voltage type. The coupling capacitor was installed directly on the floating shield of *VI*. Moreover, to measure the pattern and apparent charge of partial discharge according to the vacuum degree, phase resolved partial discharge (PRPD) for AC partial discharge and pulse sequence analysis (PSA) for DC partial discharge were adopted. It is found that maintenance should be performed when the vacuum degree is in the range of  $10^{-3} \sim 10^{-2}$  torr regardless of the voltage type. Moreover, the usefulness of the technology is higher at AC voltage than at DC voltage.

**INDEX TERMS** AC, DC, distribution class, dielectric strength, partial discharge, PRPD, PSA, monitoring, maintenance criteria, vacuum interrupter.

## I. INTRODUCTION

The trend of the global power market is eco-friendly, and research and development of renewable energy and distributed resources are progressing. Accordingly, research on eco-friendly insulation materials such as epoxy resin, dry air and Novec 4710 to replace the sulfur hexafluoride ( $\text{SF}_6$ ) gas, that, is typically applied to high voltage apparatus, is being actively conducted [1]–[3].

As one of the eco-friendly apparatus, a solid insulation high voltage apparatus comprising epoxy resin, such as a load break switch (LBS), vacuum circuit breaker (VCB) and solid insulated switchgear (SIS), is commonly installed in a distribution class power system. For a high reliability of solid

insulation high voltage apparatus, a *VI* is installed inside the housing [4]. *VI* maintains a high vacuum degree of  $10^{-7}$  torr, and has excellent insulation and arc extinguishing characteristics. In the long term operation of a distribution class solid insulation high voltage apparatus, the vacuum degree of *VI* will deteriorate because of gases emitted by arc heat, leakage through joints, ceramic cracking, and manufacturing defects. As a result, the dielectric strength of the *VI* rapidly decreases. Fig. 1 shows the Paschen curve for dry air. The dielectric strength of dry air starts to increase dramatically as the air pressure drops below approximately 10 Pa.

Fig. 2 shows the structure of *VI* and the occurrence of partial discharge. Both the fixed and moving contacts are enclosed in *VI*, which create a current interruption by causing the arc discharge to extinguish naturally in the vacuum. The arc charge is generated by opening an electrical path between

The associate editor coordinating the review of this manuscript and approving it for publication was Ye Zhou<sup>ID</sup>.

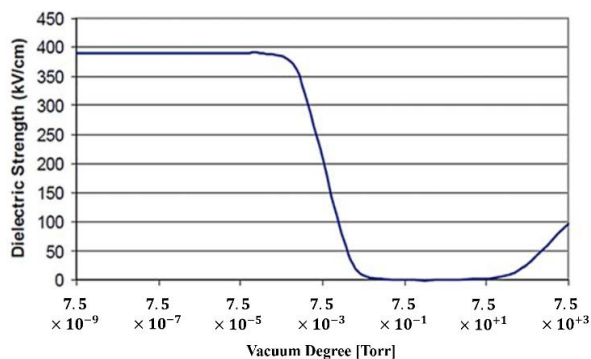


FIGURE 1. Paschen curve for dry air.

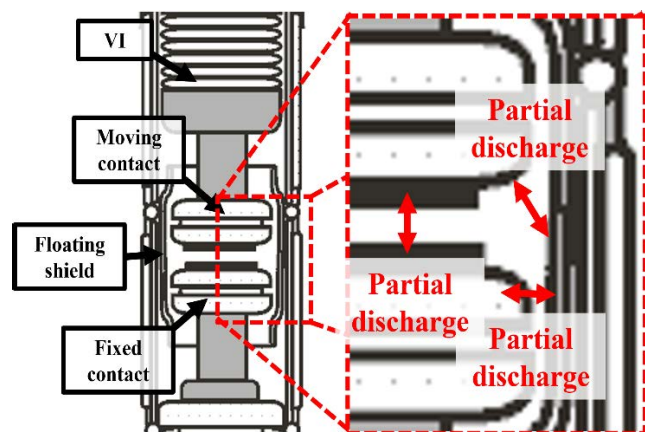


FIGURE 2. Structure of VI and the occurrence of partial discharge.

the electrodes. As the vacuum degree inside VI decreases, the dielectric strength decreases, and partial discharge occurs between the contact and floating shield, and between the contacts. The resulting dielectric problems causes electrical accidents in a solid insulation high voltage apparatus. It is important to select an appropriate VI maintenance criteria for monitoring the vacuum degree.

Currently, monitoring of the VI inside the solid insulation apparatus installed in the distribution class power system is not possible. Moreover, studies on insulation deterioration attributed to the decrease in vacuum degree have been conducted; However, other, important factors, such as the maintenance criteria, have not been investigated. Moreover, most studies have used AC voltage, not DC voltage. Prior to the research under AC voltage carried out in [5]–[13], the current method for detecting the vacuum degree inside a VI is by measuring the magnitude of DC leakage current between the VI contacts; however, this method can be applied when the VI exists alone, and cannot be applied during operation. The electromagnetic wave, discharge light intensity, and discharge sound as partial discharge characteristics were examined; however, the lowest detected pressure was approximately 1 Pa. Additionally, the power frequency withstand voltage test is widely adopted by power equipment

maintenance personnel in the on-site vacuum measurement of VCB; however, this method does not produce the specific vacuum degree value, only a simple indication of good or bad. The magnetron method has also been adopted by electric power companies for on-site measurement. Both methods require taking the VCB out of service, and the maintenance is complex. Therefore, in this paper, AC and DC partial discharge were compared by monitoring the vacuum degree in a distribution class vacuum interrupter to propose the maintenance criteria according to voltage type. For efficient maintenance of VI, the vacuum degree at which the dielectric strength rapidly decreases was confirmed according to voltage type. Moreover, to improve the accuracy of the signal detection of a partial discharge, the coupling capacitor was installed directly on the floating shield of VI. To measure the pattern and apparent charge of the partial discharge according to the vacuum degree, PRPD for AC partial discharge and PSA for DC partial discharge were adopted. Through this, efficient maintenance criteria for distribution class VI for each voltage type were proposed.

## II. DIELECTRIC CHARACTERISTICS ACCORDING TO VACUUM DEGREE INSIDE A VI

Dielectric experiments were performed according to the vacuum degree to select the effective maintenance criteria of a VI installed inside a solid insulation high voltage apparatus. Fig. 3 shows the schematic drawing of the dielectric experiment according to vacuum degree inside a VI under an AC

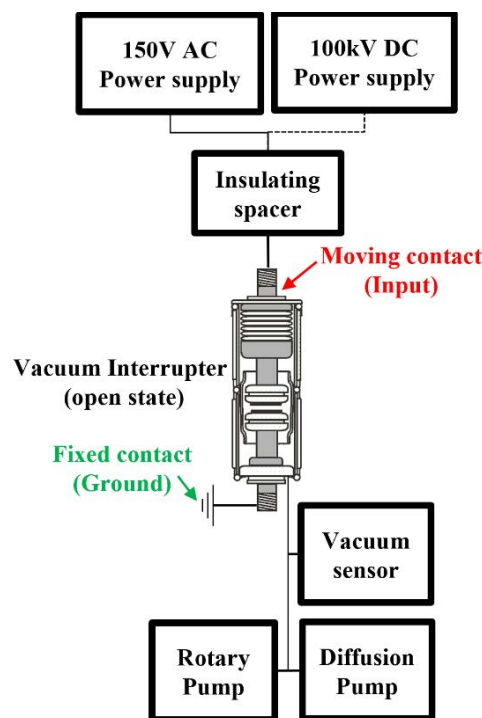


FIGURE 3. Schematic drawing of the dielectric experiment according to vacuum degree inside a VI under AC voltage and DC voltage.

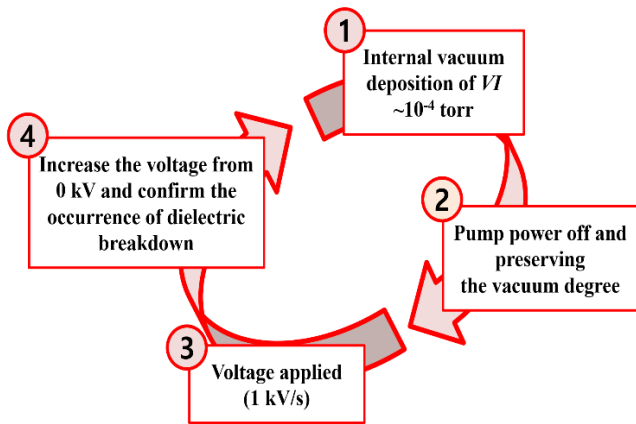


FIGURE 4. Experiment method on dielectric experiment.

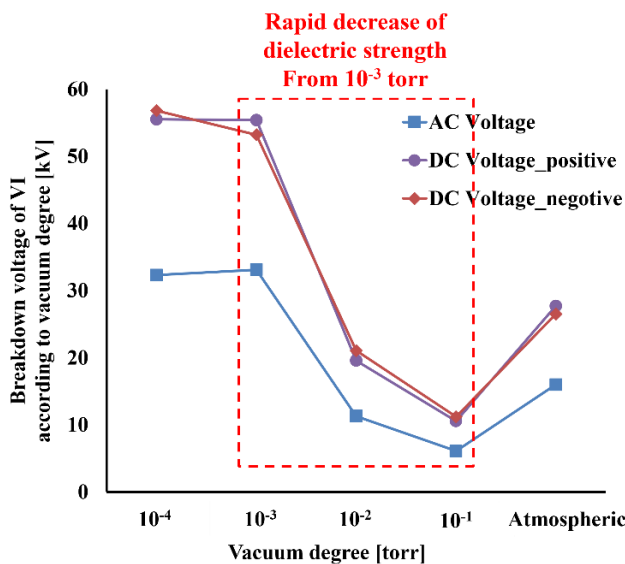


FIGURE 5. Breakdown characteristics of VI according to vacuum degree.

voltage and DC voltage. As shown in Fig. 3, an AC power supply with a capacity of 150 kV (and a cut-off current of 50 mA) and a DC power supply with a capacity of 100 kV (and a cut-off current of 21 mA) were used for the dielectric experiment according to the vacuum degree in VI. The combination of a rotary pump and diffusion pump was used to create a high vacuum. The diffusion pump uses the HiPace 300 of Pfeiffer Vacuum Co.Ltd. HiPace 300 is capable of vacuum deposition up to  $3.75 \times 10^{-10}$  torr. In addition, vacuum sensor was used to check the vacuum degree of the VI. The vacuum sensor uses the PKR 251 of Pfeiffer Vacuum Co.Ltd. PKR 251 is capable of measuring vacuum up to  $5 \times 10^{-9}$  torr. An insulating spacer made by MC nylon was installed to impart electrical stability between the vacuum sensor and VI. VI is in the open state, and the distance between the contacts is 12 mm. An input voltage was applied to the moving contact and grounded to the fixed contact. Fig. 4 shows the experiment method on dielectric experiment. The vacuum degree

of VI was controlled up to  $10^{-4}$  torr. Then, the power to the pumps was then turned off, and the dielectric experiments were conducted while preserving the vacuum degree inside VI for each condition. A total of five VIs were used in the dielectric experiment. A total of 10 experiments were conducted for each VI, and the average breakdown voltages were calculated. Fig. 5 shows the breakdown characteristics of VI according to the vacuum degree in VI.

In Fig. 5, “negative” and “positive” refer to the negative and positive polarity of the DC voltage. The red rectangle represents the section where a rapid decrease in dielectric strength occurs. As shown Fig. 5, as the vacuum degree of VI decreased from  $10^{-4}$  torr to  $10^{-1}$  torr, the dielectric strength decreased. However, as the vacuum degree is further decreased from  $10^{-1}$  torr to the atmospheric pressure, the dielectric strength increased. The dielectric strength of the vacuum decreased rapidly from  $10^{-3}$  torr. Therefore, the VI maintenance should be conducted when the vacuum degree is in the range of  $10^{-3} \sim 10^{-2}$  torr.

### III. CAPACITY CALCULATION AND INSTALLATION OF THE COUPLING CAPACITOR

To improve the accuracy of the signal detection of the partial discharge generated according to vacuum degree inside VI, the coupling capacitor was installed directly on the floating shield, as shown Fig. 6 [14]. Fig. 7 shows the equivalent circuit on the structure when coupling capacitor is directly installed in VI [14]. As shown in Fig. 6 and 7,  $V_0$ ,  $V_a$ , and  $V_s$  represent the input voltage between the contact and ground, the voltage between the contact and floating shield, and the voltage and between the floating shield and ground, respectively.  $C_a$ ,  $C_s$ , and  $C_c$  represent the capacitance between

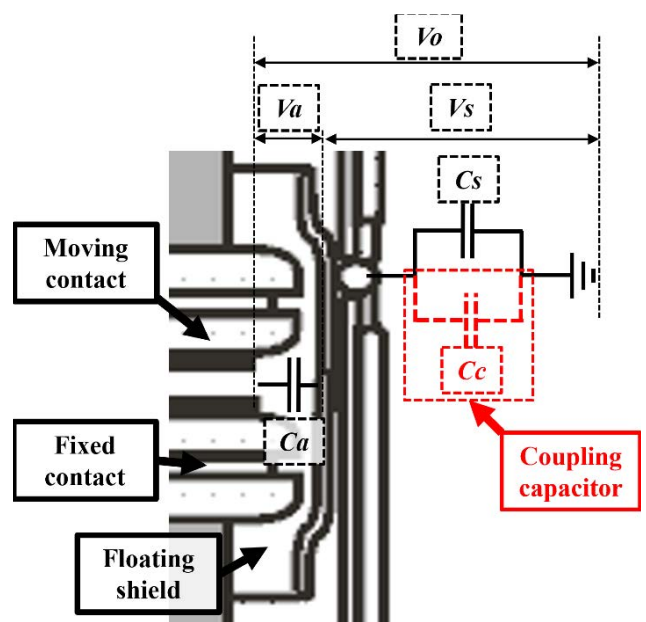


FIGURE 6. Structure when the coupling capacitor is directly insulated in VI.

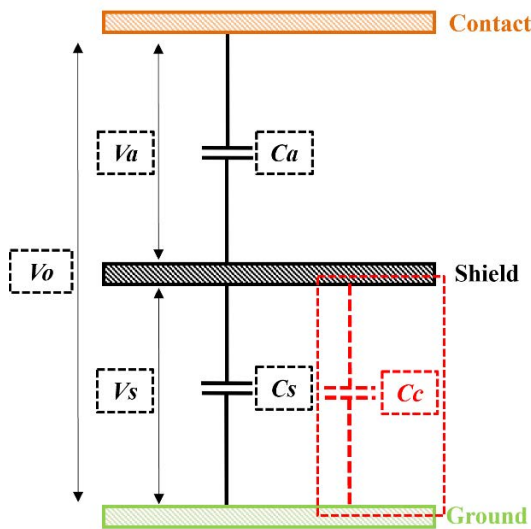


FIGURE 7. Equivalent circuit on the structure when the coupling capacitor is directly insulated in VI.

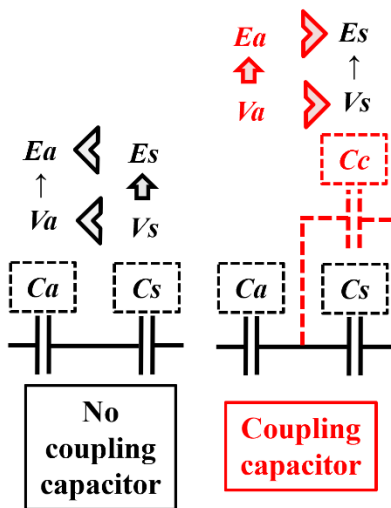


FIGURE 8. Effect of coupling capacitor.

the contact and floating shield, the capacitance between the floating shield and ground, and the coupling capacitance, respectively. The capacitance components, such as  $C_a$  and  $C_s$ , are generated between the contact and floating shield and between the floating shield and ground. While the solid insulation apparatus is in operation, the VI is in the closed state. Therefore, it is very important to detect the partial discharge signal between the contact and the floating shield rather than between the two contacts. To improve the accuracy of the signal detection of the partial discharge, the capacitance component present inside VI should be adjusted.  $C_a$  is generally larger than  $C_s$ , and  $V_a$  becomes smaller than  $V_s$ . Therefore, the electric field intensity at  $V_a$  ( $E_a$ ) becomes smaller than the electric field intensity at  $V_s$  ( $E_s$ ), and the signal of partial discharge between the contact and floating shield may not

be accurately measured. The voltage components for before the coupling capacitor were installed are expressed by Eq. (1) and (2).

$$V_a = (C_s / (C_a + C_s)) V_0 \quad (1)$$

$$V_s = (C_a / (C_a + C_s)) V_0 \quad (2)$$

If  $C_c$  with a larger capacity than  $C_a$  is installed in VI, like Fig. 7,  $C_c$  and  $C_s$  are generated in parallel, and  $C_c$  is added to  $C_s$ . Fig. 8 shows the effect of coupling capacitor. As shown Fig. 8,  $V_a$  becomes larger than  $V_s$ , and  $E_a$  becomes larger than the  $E_s$ . The voltage components for after the coupling capacitor were installed are expressed by Eq. (3) and (4).

$$V_a = ((C_s + C_c) / (C_a + C_s + C_c)) V_0 \quad (3)$$

$$V_s = (C_a / (C_a + C_s + C_c)) V_0 \quad (4)$$

To improve the accuracy of the signal detection of partial discharge, it is very important to install  $C_c$  which has a larger capacity than  $C_a$ , into VI. The equation for calculating  $C_a$  is expressed in (5) [14].

$$C_a = (2 \times \pi \times \epsilon_0 \times H) / (\ln (R_2 / R_1)) \quad (5)$$

In Eq. (5),  $H$  represents the contact length,  $R_1$  and  $R_2$  represent the outside diameter of the contact and the inner diameter of the metal shield respectively, and  $\epsilon_0$  represents the relative permittivity of a vacuum. As a result,  $C_a$  between the contact and floating shield of VI is approximately 26 pF. In this paper, to analyze the partial discharge characteristics according to the vacuum degree inside VI, a  $C_c$  of 38 pF was installed in VI.

#### IV. AC AND DC PARTIAL DISCHARGE CHARACTERISTICS ACCORDING TO THE VACUUM DEGREE INSIDE VI

##### A. AC PARTIAL DISCHARGE CHARACTERISTICS

The partial discharge experiments were performed to analyze partial discharge characteristics according to the vacuum degree. Fig. 9 shows a schematic drawing of the partial discharge experiment according to the vacuum degree inside the VI under AC voltage. Partial discharge experiments were conducted in a shielded room. As with the dielectric experiment, the combination of a rotary pump and diffusion pump was used to create a high vacuum, and vacuum sensor was used to check the vacuum degree of the VI. An insulating spacer made by MC nylon was installed to impart electrical stability between the vacuum sensor and VI. An AC power supply with a capacity of 50 kV (and a cut-off current of 25 mA) and the partial discharge measurement system are used. The partial discharge measurement system uses the LDS-6 of Doble Lemke Co.Ltd. LDS-6 has a measurement frequency range of 30 ~ 470 Hz, a single pulse resolution of  $\leq 100$  kHz repetition rate, and is in accordance with IEC 60270. In addition, the PRPD method was applied because the partial discharge characteristics were analyzed under AC voltage. The coupling capacitor was directly connected to the floating shield of the VI. At this time, VI is in the closed state

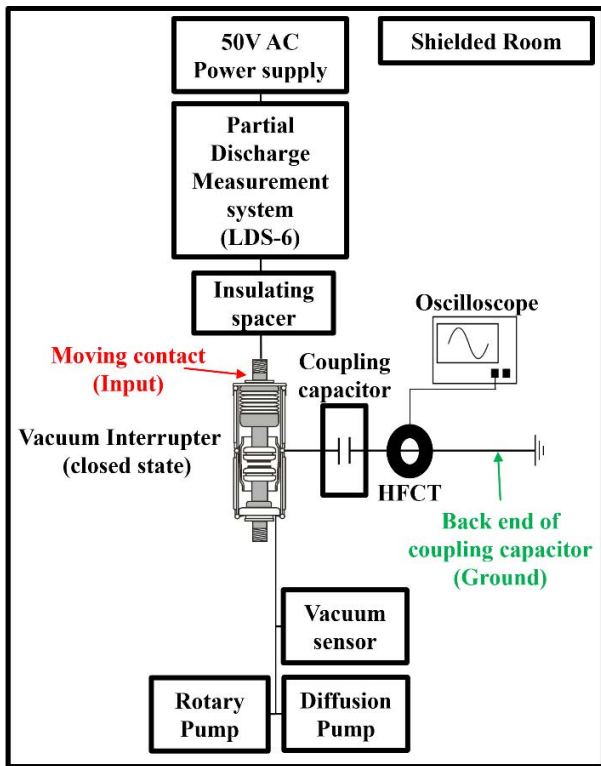


FIGURE 9. Schematic drawing of the partial discharge experiment according to the vacuum degree inside VI under AC voltage.

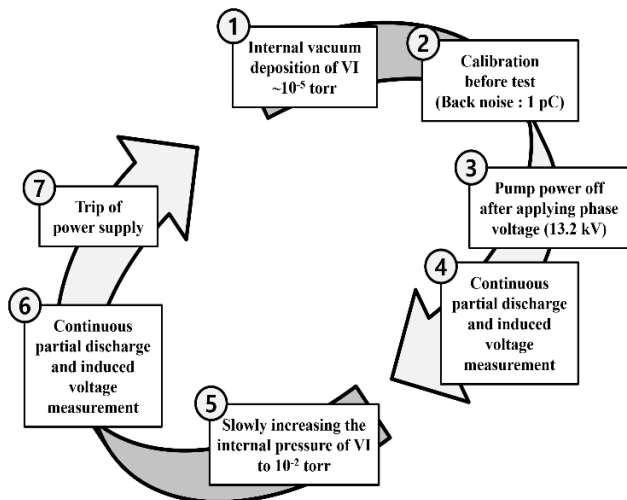


FIGURE 10. Experiment method on AC partial discharge experiment.

because it can simulate the operation condition of VI in a solid insulation apparatus. The input voltage was applied to the moving contact and the back end of the coupling capacitor was grounded. The time division and voltage division of the oscilloscope were set to  $5 \mu s$  and  $30 mV$ , respectively. A total of two VIs with the same electrical properties, 130 mm in diameter and 110 mm in height, were used. Fig. 10 shows the experiment method on AC partial discharge experiment. As shown Fig. 10, a high vacuum degree of  $10^{-5}$  torr inside

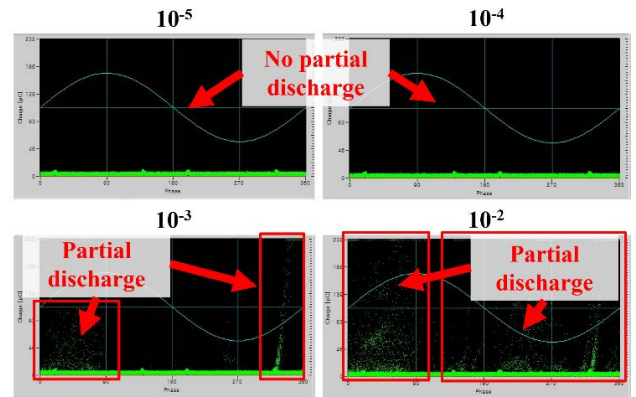


FIGURE 11. Pattern of partial discharge measured through PRPD method under AC voltage.

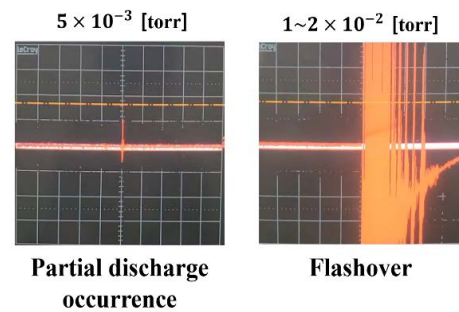


FIGURE 12. Induced voltage waveform measured through a coupling capacitor under AC voltage.

the VI was created and the rotary pump and diffusion pump were turned off. At this time, the calibration of the partial discharge measurement system was performed before the experiment, and the back noise was set to 1 pC. An AC voltage of 13.2 kV with 60 Hz was continuously applied for the phase voltage of 22.9 kV, because the distribution class voltage in the Republic of Korea is 13.2 kV [14], [16]. The vacuum degree inside the VI was gradually decreased to  $10^{-2}$  torr, and the partial discharge was measured. Moreover, the waveform of the induced voltage flowing through the coupling capacitor was checked with an oscilloscope. An experiment was performed for 50 minutes in which the vacuum degree was maintained from  $10^{-5}$  torr to  $10^{-2}$  torr, and the experiment for each VI was performed a total of 6 times.

Fig. 11 shows the pattern of the partial discharge measured through the PRPD method under AC voltage. Fig. 12 shows the induced voltage waveform measured through the coupling capacitor under AC voltage. As shown Fig. 11 and 12, the partial discharge did not occur in the range from  $10^{-5}$  torr to  $10^{-4}$  torr. However, partial discharge occurred from  $10^{-3}$  torr, and flashover occurred at  $10^{-2}$  torr. Therefore, the dielectric strength decreased from  $10^{-3}$  torr, similar to the dielectric characteristics as a function of the vacuum degree. Fig. 13 and 14 show the AC partial discharge characteristics of VI 1 and 2. “Experiments 1 ~ 6” represent the number of experiments for each VI, and “VI 1 and 2” represent two

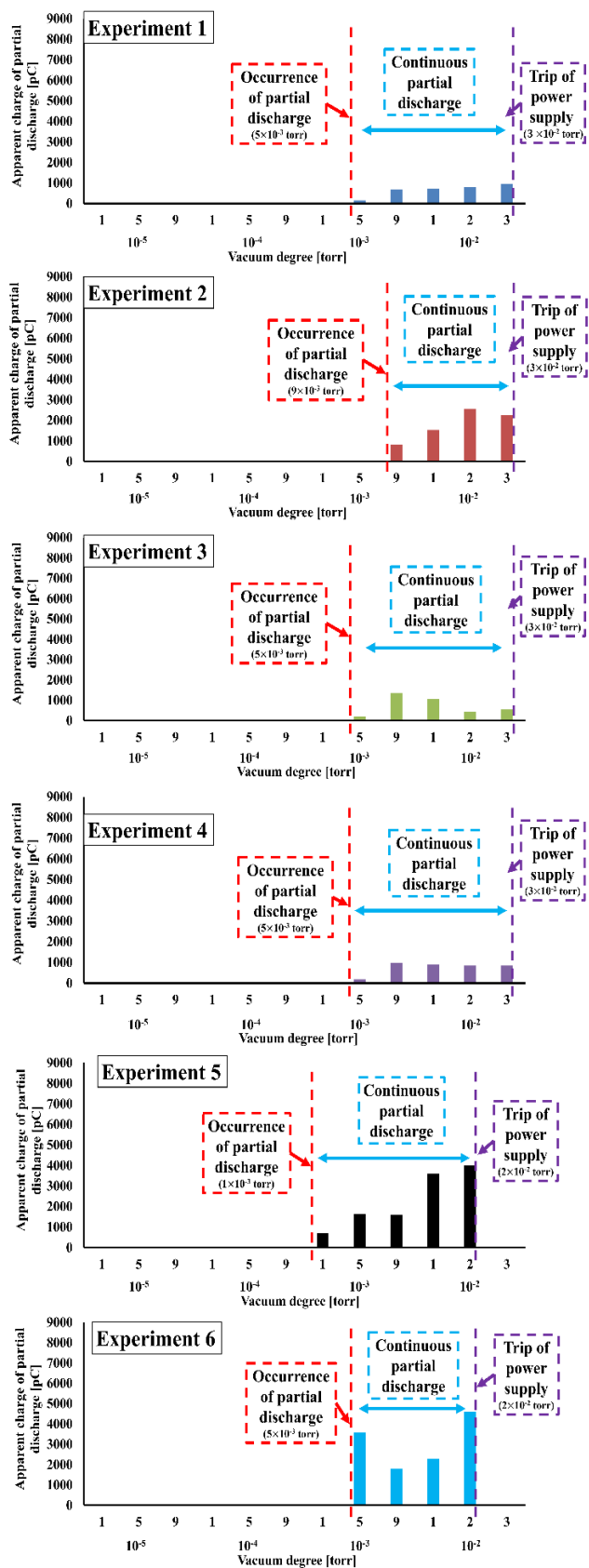


FIGURE 13. AC partial discharge characteristics of VI 1.

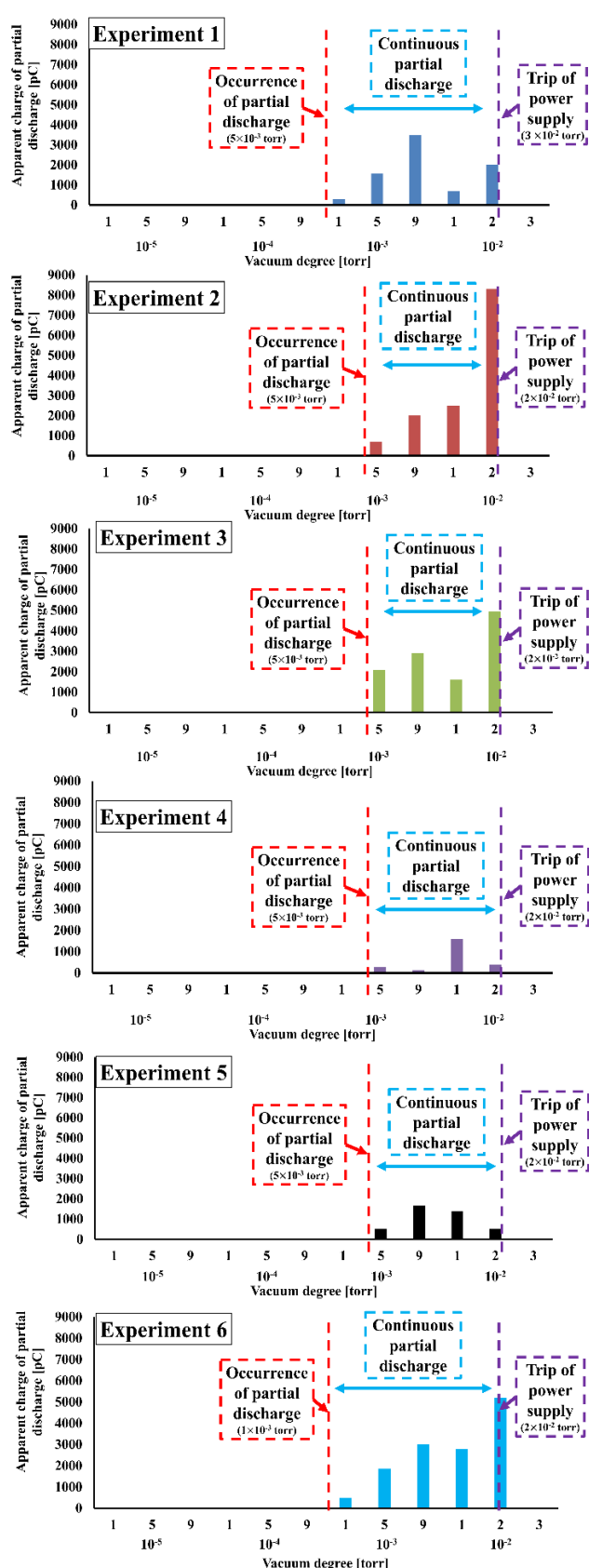


FIGURE 14. AC partial discharge characteristics of VI 2.

**TABLE 1.** Maximum and minimum apparent charge in each experiment and VI under AC voltage.

	VI 1	VI 2
Peak apparent charge [pC]	4,000	8,300
(vacuum degree / experiment number)	( $10^{-2}$ torr / fifth)	( $10^{-2}$ torr / second)
Minimum apparent charge [pC]	158	126
(vacuum degree / experiment number)	( $10^{-3}$ torr / first)	( $10^{-3}$ torr / forth)

VIs with having the same structural and electrical properties. As shown in Fig. 13 and 14, in both VI 1 and VI 2, the AC partial discharge was occurred from  $10^{-3}$  torr and maintained continuously until maximum  $3 \times 10^{-2}$  torr. After that, a flashover occurs between the contact and the floating shield, and the power supply trips. However, the apparent charge of the AC partial discharge was generated with a different magnitude for each vacuum degree, and different partial discharge characteristics appeared for each experiment and VIs. Table 1 shows the maximum and minimum apparent generated charge in each experiment and VI under AC voltage. As shown in Table 1, in case of VI 1, the maximum apparent charge was 4,000 pC, which was generated in the fourth experiment, and the minimum apparent charge was 158 pC, which was generated in the first experiment. In case of VI 2, the maximum apparent charge was 8,300 pC, which was generated in the second experiment, and the minimum apparent charge was 126 pC, which was generated in the forth experiment. The vacuum degree at which partial discharge occurs is similar, but the point at which discharge occurs between the conductor and floating shield is different. Therefore, partial discharge characteristics are generated differently for each experiment and VI of the same characteristics.

To select an effective maintenance criteria for VI, it is important to select the minimum value, and not the maximum, as the trigger value for the detection of electrical accidents. In this paper, the minimum value as the trigger value of AC partial discharge is proposed as 126 pC.

**B. DC PARTIAL DISCHARGE CHARACTERISTICS**

Fig. 15 shows a schematic drawing of the partial discharge experiment according to vacuum degree inside the VI under DC voltage. As with the AC partial discharge experiment, the DC partial discharge experiments were conducted in a shielded room. A combination of a rotary pump and a diffusion pump was used to create a high vacuum, and a vacuum sensor was used to check the vacuum degree of the VI. An insulating spacer was installed to impart electrical stability between the vacuum sensor and VI. A DC power supply with a capacity of 100 kV (cut-off current of 21 mA) and full wave rectifier was used. The partial discharge measurement system uses PDMS of SM&D Co.Ltd. The DC partial

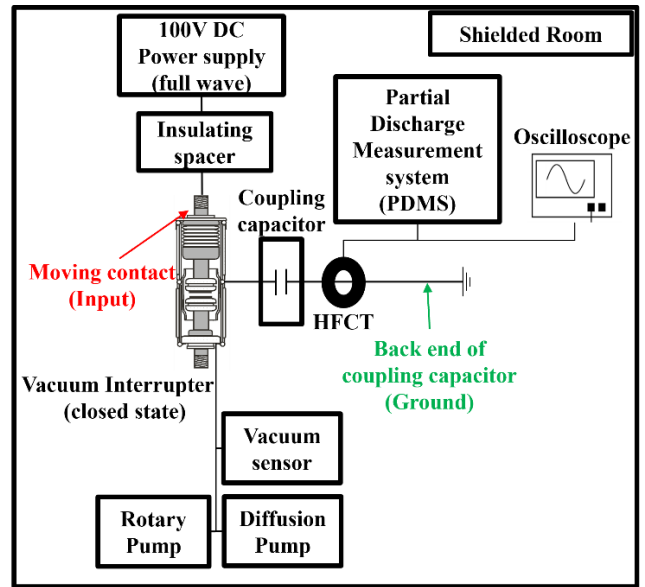


**FIGURE 15.** Schematic drawing of the partial discharge experiment according to vacuum degree inside the VI under DC voltage.

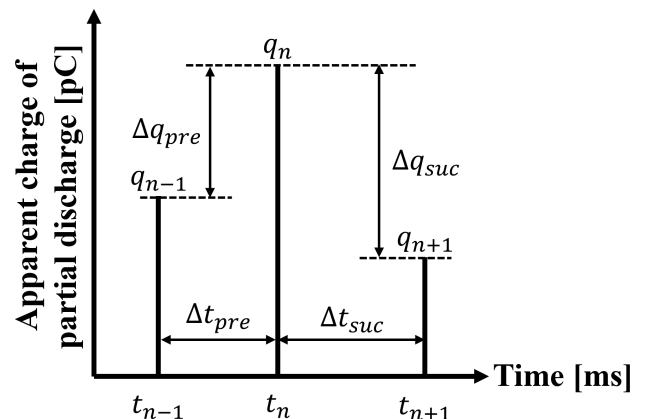


**FIGURE 16.** Basic parameters of PSA.

discharge was not clearly defined in the IEC 60270 [17]. When the DC voltage increased (switching on state), a capacitive electric field, such as AC electric field, is generated because polarization occurs in the insulation material. In this paper, the DC partial discharge was defined as the partial discharge generated in a resistive electric field (steady state). Moreover, the apparent charge of DC partial discharge can not be measured using the PRPD method like AC voltage because DC voltage has no phase information. Therefore, the DC partial voltage was measured by the PSA method, a method for analyzing the correlation between sequentially generated pulses. The PSA method uses a technique to analyze the correlation between the previous and successive discharge pulses to verify the space charge effect caused by the previous discharge pulse [18]. Fig. 16 shows the basic parameter of PSA. “ $q_n$ ,” “ $q_{n-1}$ ,” and “ $q_{n+1}$ ” represent the magnitude of discharge, pervious discharge, and successive

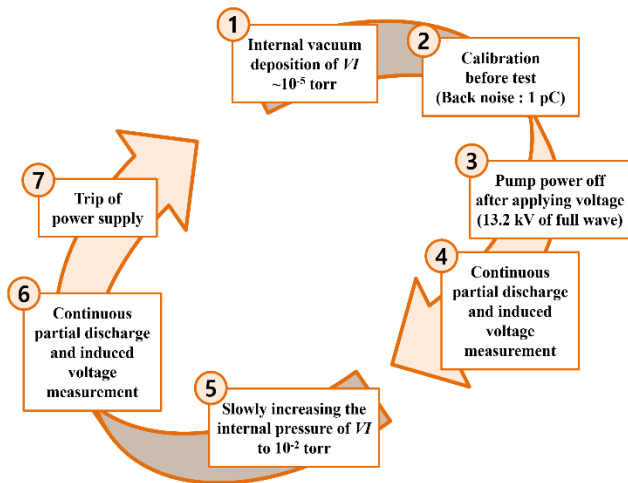


FIGURE 17. Experiment method on DC partial discharge experiment.

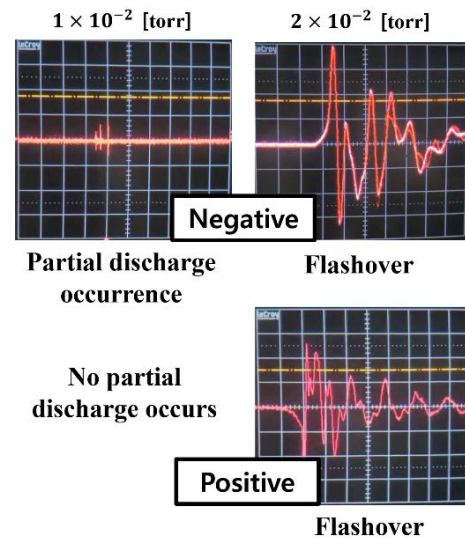


FIGURE 19. Induced voltage waveform measured using the coupling capacitor under DC voltage.

and voltage division of the oscilloscope were set to  $0.1 \mu\text{s}$  and  $10 \text{ mV}$ , respectively. A total of two VIs with the same electrical properties,  $130 \text{ mm}$  in diameter and  $110 \text{ mm}$  in height, were used. Fig. 17 shows the experiment method on DC partial discharge experiment. The experiment method is similar to the AC partial discharge experiment. As shown Fig. 17, a high vacuum degree of  $10^{-5}$  torr inside the VI was created and the rotary pump and diffusion pump were turned off. At this time, the calibration of the partial discharge measurement system was performed before the experiment, and back noise was set to  $1 \text{ pC}$ . A high vacuum degree of  $10^{-5}$  torr was created inside VI and the rotary pump and diffusion pump were turned off. A DC voltage of  $13.2 \text{ kV}$ , which is the same as the applied voltage during the AC partial discharge experiment, was then applied. The vacuum degree inside VI was gradually decreased to  $10^{-2}$  torr, and the partial discharge was measured. The waveform of the induced voltage flowing through the coupling capacitor was checked with an oscilloscope. An experiment was performed for 50 minutes in which vacuum degree was maintained from  $10^{-5}$  torr to  $10^{-2}$  torr, and the experiments for VI 1 and VI 2 were performed a total of 10 times and a total of 7 times, respectively. Also, the experiment was performed with the same number of experiments for each voltage polarity.

Fig. 18 shows the pattern of the partial discharge measured using the PSA method under DC voltage. Fig. 19 shows the induced voltage waveform measured using the coupling capacitor under DC voltage. “Positive” and “Negative” represent the positive and negative polarity of the DC voltage. As shown in Fig. 18 and 19, the induced voltage and partial discharge did not occur in the range from  $10^{-5}$  torr to  $10^{-3}$  torr. In the positive polarity, the induced voltage and partial discharge occurred from  $10^{-2}$  torr, and flashover occurred immediately. However, in the negative polarity, after the

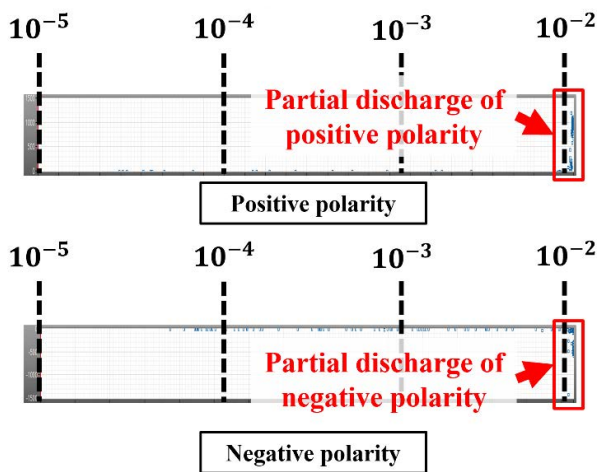


FIGURE 18. Pattern of the DC partial discharge measured using the PSA method under DC voltage.

discharge, respectively. “ $t_n$ ,” “ $t_{n-1}$ ,” and “ $t_{n+1}$ ” represent the discharge time, previous discharge time, and successive discharge time, respectively. “ $\Delta q_{pre}$ ” and “ $\Delta t_{pre}$ ” represent the previous discharge difference between  $q_n$  and  $q_{n-1}$  and the previous discharge time difference between  $q_n$  and  $q_{n-1}$ , respectively. “ $\Delta q_{suc}$ ” and “ $\Delta t_{suc}$ ” represent the successive discharge difference between  $q_{n+1}$  and  $q_n$  and the successive discharge time difference between  $q_n$  and  $q_{n-1}$ , respectively. The main parameters used in the PSA method are  $\Delta t$  and  $\Delta q$  [18]. There are a total of four methods for measuring DC partial discharge using the PSA method :  $q_n$  vs  $\Delta t_{pre}$ ,  $q_n$  vs  $\Delta t_{suc}$ ,  $\Delta t_{pre}$  vs  $\Delta t_{suc}$ , and  $\Delta q_{pre}$  vs  $\Delta q_{suc}$  [18]. To measure the DC partial discharge according to the vacuum degree inside VI, the  $\Delta q_{pre}$  vs  $\Delta q_{suc}$  method was used. The coupling capacitor was directly connected to the floating shield of VI. VI is in the closed state. Additionally, the input voltage was applied to moving contact and the back end of coupling capacitor was grounded. The time division



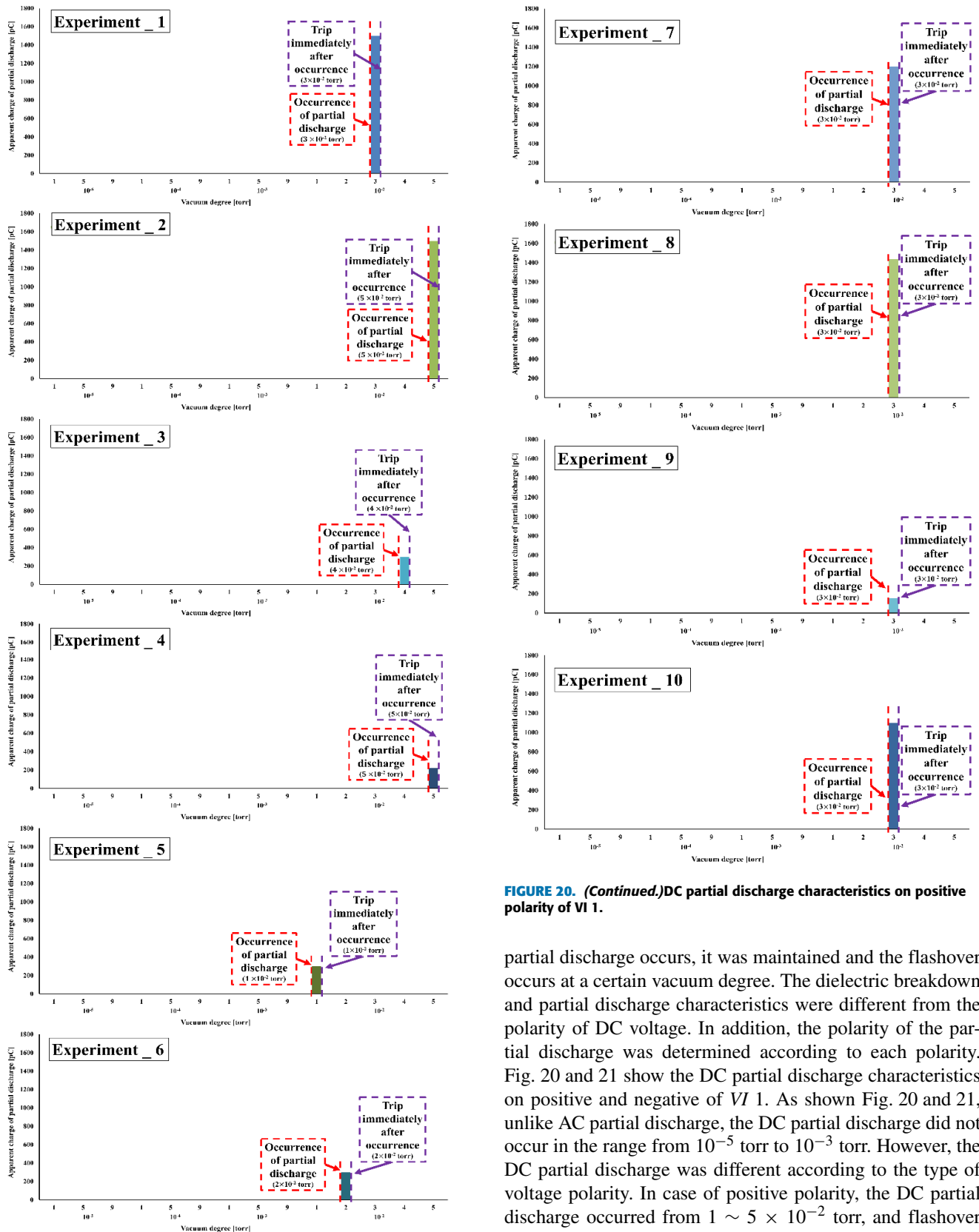


FIGURE 20. DC partial discharge characteristics on positive polarity of VI 1.

FIGURE 20. (Continued.)DC partial discharge characteristics on positive polarity of VI 1.

partial discharge occurs, it was maintained and the flashover occurs at a certain vacuum degree. The dielectric breakdown and partial discharge characteristics were different from the polarity of DC voltage. In addition, the polarity of the partial discharge was determined according to each polarity. Fig. 20 and 21 show the DC partial discharge characteristics on positive and negative of VI 1. As shown Fig. 20 and 21, unlike AC partial discharge, the DC partial discharge did not occur in the range from  $10^{-5}$  torr to  $10^{-3}$  torr. However, the DC partial discharge was different according to the type of voltage polarity. In case of positive polarity, the DC partial discharge occurred from  $1 \sim 5 \times 10^{-2}$  torr, and flashover immediately occurs between the contact and the floating shield. In case of negative polarity, the DC partial discharge

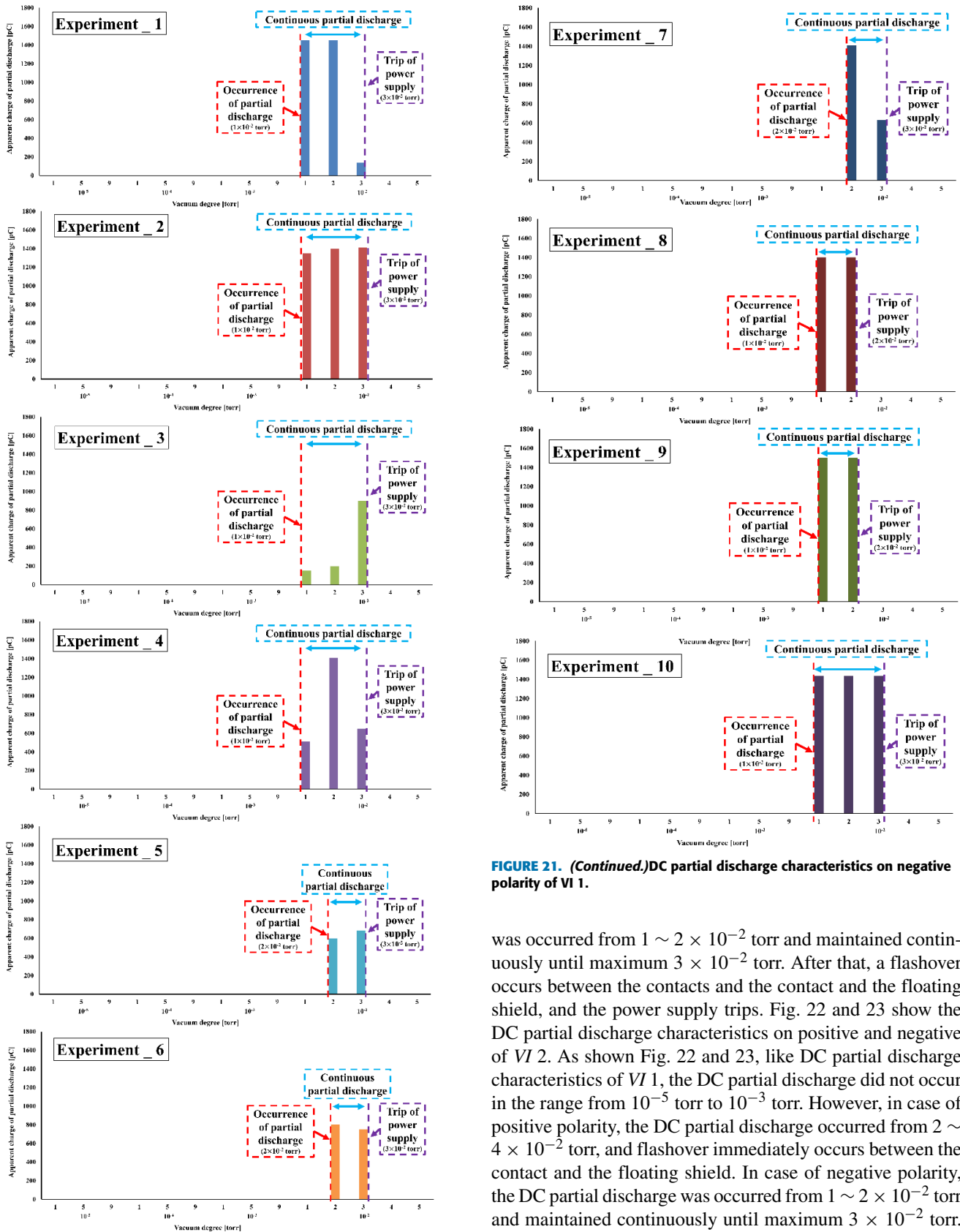


FIGURE 21. (Continued.) DC partial discharge characteristics on negative polarity of VI 1.

was occurred from  $1 \sim 2 \times 10^{-2}$  torr and maintained continuously until maximum  $3 \times 10^{-2}$  torr. After that, a flashover occurs between the contacts and the contact and the floating shield, and the power supply trips. Fig. 22 and 23 show the DC partial discharge characteristics on positive and negative of VI 2. As shown Fig. 22 and 23, like DC partial discharge characteristics of VI 1, the DC partial discharge did not occur in the range from  $10^{-5}$  torr to  $10^{-3}$  torr. However, in case of positive polarity, the DC partial discharge occurred from  $2 \sim 4 \times 10^{-2}$  torr, and flashover immediately occurs between the contact and the floating shield. In case of negative polarity, the DC partial discharge was occurred from  $1 \sim 2 \times 10^{-2}$  torr and maintained continuously until maximum  $3 \times 10^{-2}$  torr. After that, a flashover occurs between the contacts and the contact and the floating shield, and the power supply trips.

FIGURE 21. DC partial discharge characteristics on negative polarity of VI 1.

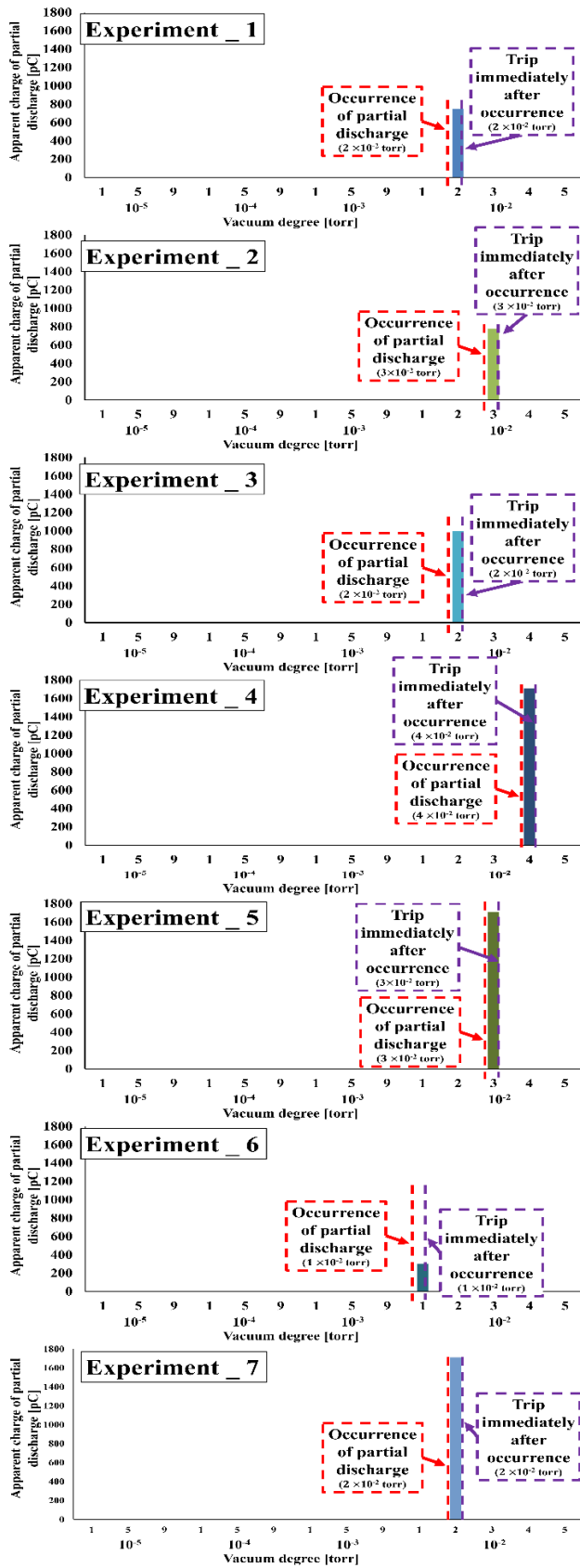


FIGURE 22. DC partial discharge characteristics on positive polarity of VI 2.

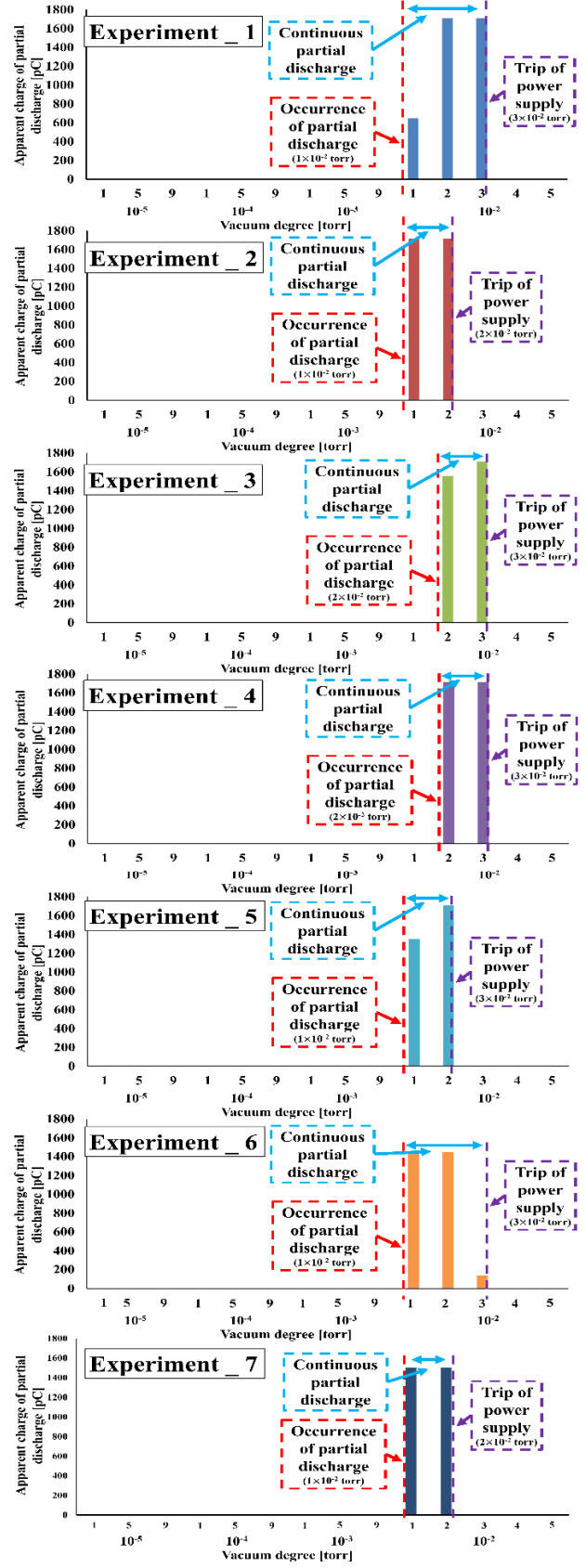


FIGURE 23. DC partial discharge characteristics on negative polarity of VI 2.

**TABLE 2. Maximum and minimum apparent charge in each experiment and VI under DC voltage.**

		VI 1	VI 2
Peak apparent charge [pC] (vacuum degree / experiment number)	Positive	1,712 (10 <sup>-2</sup> torr / second, fourth, and seventh)	1,500 (10 <sup>-2</sup> torr / first, and second)
	Negative	1,500 (10 <sup>-2</sup> torr / ninth)	1,500 (10 <sup>-2</sup> torr / first, and second)
Minimum apparent charge [pC] (vacuum degree / experiment number)	Positive	100 (10 <sup>-2</sup> torr / ninth)	96 (10 <sup>-3</sup> torr / sixth)
	Negative	140 (10 <sup>-2</sup> torr / first)	140 (10 <sup>-3</sup> torr / sixth)

It is confirmed that the maximum and minimum apparent charges are different for each experiment, VIs, and voltage polarity. Moreover, the time interval between DC partial discharge and flashover was very short than that of AC partial discharge. Therefore, the DC partial discharge characteristics were weaker in the negative polarity than in the positive polarity according to the vacuum degree inside VI. It was found that the maintenance of VI is more difficult at DC voltage than AC voltage. Table 2 shows the maximum and minimum apparent generated charge in each experiment and VI under DC voltage. As shown in Table 2, in case of VI 1, the maximum apparent charge of positive polarity was 1,712 pC, which was generated in the second, fourth, and seventh experiments, and the maximum apparent charge of negative polarity was 1,500 pC, which was generated in the first and second experiments. Also, the minimum apparent charge of positive polarity was 100 pC, which was generated in the ninth experiment, and the minimum apparent charge of negative polarity was 140 pC, which was generated in the first experiment. In case of VI 2, the maximum apparent charge of positive and negative polarity was 1,500 pC, which was generated in the first and second experiments. Also, the minimum apparent charge of positive polarity was 96 pC, which was generated in the sixth experiment, and the minimum apparent charge of negative polarity was 140 pC, which was generated in the sixth experiment. Like AC partial discharge characteristics, the partial discharge characteristics are generated differently for each experiment and VI of the same characteristics because the point at which discharge occurs between the conductor and floating shield is different. In additions, since the time interval of DC voltage is much shorter than that of AC voltage, it is very important to select the trigger value.

In this paper, the minimum value of DC partial discharge as the trigger value was proposed as 96 pC for positive polarity and 140 pC for negative polarity.

**V. PROPOSAL OF THE MAINTENANCE CRITERIA OF VI ACCORDING TO AC AND DC VOLTAGE**

In this paper, for efficient maintenance of VI, AC and DC partial discharge were compared by monitoring of the vacuum

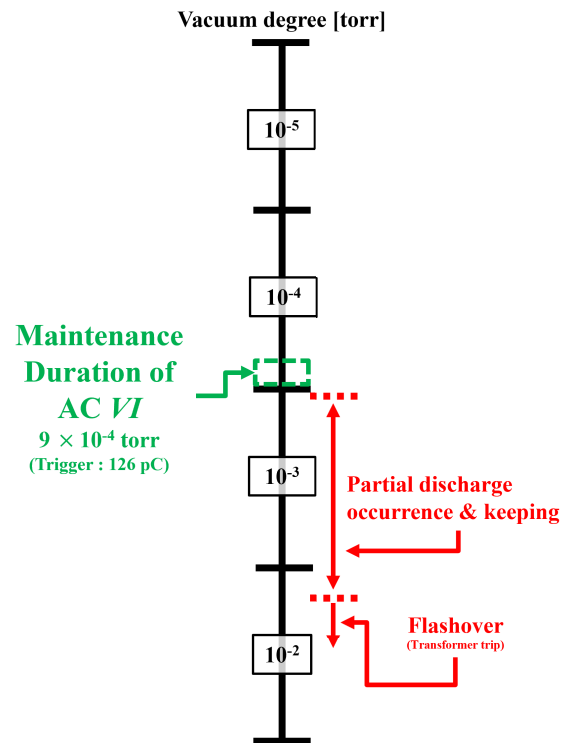


**FIGURE 24. Partial discharge and flashover characteristics and proposal of maintenance criteria according to vacuum degree under AC voltage.**

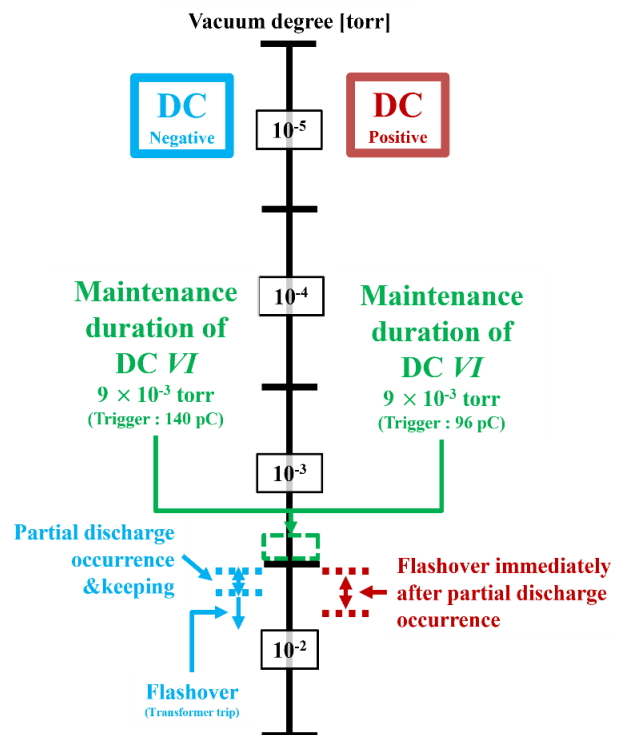


**FIGURE 25. Partial discharge and flashover characteristics and proposal of maintenance criteria according to vacuum degree under DC voltage.**

degree in a distribution class VI to propose maintenance criteria according to voltage type. Through this, for efficient

maintenance, maintenance criteria of VI for each voltage type are presented.

Fig. 24 shows the partial discharge and flashover characteristics and proposal of the maintenance criteria according to vacuum degree under AC voltage. Fig. 25 shows the partial discharge and flashover characteristics and proposal of the maintenance criteria according to vacuum degree under DC voltage. As shown in Fig. 24 and 25, although AC partial discharge occurs earlier than DC partial discharge, the time interval between the partial discharge and flashover generated at DC voltage was much shorter than that of AC voltage. Therefore, the maintenance of VI is more difficult at DC voltage than AC voltage. Regardless of voltage type, the maintenance of VI should be conducted at vacuum degree before partial discharge occurs. If the proposed trigger value according to AC and DC voltage is detected, then the dielectric strength of VI has started to decrease rapidly. Therefore, in this paper, the maintenance criteria of VI is proposed as  $9 \times 10^{-4}$  torr for AC VI, and  $9 \times 10^{-3}$  torr for DC VI, which is the vacuum degree before partial discharge occurs.

## VI. CONCLUSION

AC and DC partial discharge were compared by monitoring the vacuum degree in a distribution class VI to propose maintenance criteria according to voltage type. For efficient maintenance of VI, the vacuum degree at which the dielectric strength rapidly decreased was confirmed according to voltage type. Moreover, to improve the accuracy of the signal detection of the partial discharge, the coupling capacitor was installed directly on the floating shield of VI. To measure the pattern and apparent charge of the partial discharge according to the vacuum degree, PRPD for AC partial discharge and PSA for DC partial discharge were adopted, respectively. The results of this study are as follows:

- Regardless of voltage type, the dielectric strength of the vacuum decreased rapidly from  $10^{-3}$  torr.
- For AC voltage, the partial discharge occurred from  $1 \sim 5 \times 10^{-3}$  torr and flashover occurred after  $3 \times 10^{-2}$  torr.
- For positive polarity of DC voltage, the partial discharge occurred from  $1 \sim 5 \times 10^{-2}$  torr, and flashover occurred immediately.
- For negative polarity of DC voltage, the flashover occurs at certain vacuum degree after the partial discharge occurs at  $1 \sim 2 \times 10^{-2}$  torr.
- Partial discharge characteristics are generated differently for each experiment and VI of the same characteristics because the point at which discharge occurs between the contact and floating shield is different.
- In additions, although AC partial discharge occurs earlier than DC partial discharge, the time interval between partial discharge and flashover generated at DC voltage was much shorter than that of AC voltage.

- For efficient maintenance of VI, a maintenance criteria of VI is proposed as  $9 \times 10^{-4}$  torr for AC VI, and  $9 \times 10^{-3}$  torr for DC VI.
- The trigger value of AC VI was 126 pC, and the trigger values of DC VI was 96 pC for positive polarity and 140 pC for negative polarity.
- Therefore, the usefulness of the technology is higher at AC voltage than at DC voltage.

## REFERENCES

- [1] S. J. Dodd, N. M. Chalashkanov, J. C. Fothergill, and L. A. Dissado, "Influence of the temperature on the dielectric properties of epoxy resins," in *Proc. IEEE ICSD*, Jul. 2010, pp. 1–4, doi: [10.1109/ICSD.2010.5567945](https://doi.org/10.1109/ICSD.2010.5567945).
- [2] D. van der Born, P. H. F. Morshuis, J. J. Smit, and A. Girodet, "Negative LI breakdown behavior of electrodes with thin dielectric coatings in dry air at high pressure," in *Proc. IEEE CEIDP*, Oct. 2014, pp. 82–85, doi: [10.1109/CEIDP.2014.6995738](https://doi.org/10.1109/CEIDP.2014.6995738).
- [3] A. Xiao, J. G. Owens, J. Bonk, A. Zhang, C. Wang, and Y. Tu, "Environmentally friendly insulating gases as SF<sub>6</sub> alternatives for power utilities," in *Proc. IEEE ICEMPE*, Apr. 2019, pp. 42–48, doi: [10.1109/ICEMPE.2019.8727308](https://doi.org/10.1109/ICEMPE.2019.8727308).
- [4] C. Y. Park, D. H. Lee, J. U. Choi, and S. W. Park, "Analysis of PD characteristics depending on causes of solid insulated load break switchgear," in *Proc. CMD*, Sep. 2012, pp. 818–820, doi: [10.1109/CMD.2012.6416273](https://doi.org/10.1109/CMD.2012.6416273).
- [5] Y. W. Youn, D. H. Hwang, J. H. Sun, K. D. Song, H. R. Koh, and Y. I. Kim, "Development of measuring and analysis method for monitoring the vacuum degree in VI," in *Proc. KIEE*, 2013, pp. 1370–1371.
- [6] X. Duan, F. Li, E. Dong, M. Liao, Y. Guo, and J. Zou, "Study on inner vacuum pressure measurement system of vacuum circuit breakers," in *Proc. IEEE ICEPE-ST*, Oct. 2017, pp. 880–884, doi: [10.1109/ICEPE-ST.2017.8188970](https://doi.org/10.1109/ICEPE-ST.2017.8188970).
- [7] Y. Nakano, M. Kozako, M. Hikita, T. Tanaka, and M. Kobayashi, "Estimation of internal pressure of vacuum interrupter by measuring partial discharge current," in *Proc. ISDEIV*, Sep. 2018, pp. 611–614, doi: [10.1109/DEIV.2018.8537045](https://doi.org/10.1109/DEIV.2018.8537045).
- [8] J. Abe, T. Tanabe, T. Yano, S. Yoshida, and N. Inoue, "The electric discharge detection method in the low vacuum region of vacuum interrupter," *Electron. Commun. Jpn.*, vol. 136, no. 2, pp. 154–160, 2016.
- [9] X. Deng, W. Li, and B. Liu, "Discharge properties and diagnosis of gas pressure in vacuum interrupter," in *Proc. IEEE PEAM*, Sep. 2011, pp. 314–317, doi: [10.1109/PEAM.2011.6134952](https://doi.org/10.1109/PEAM.2011.6134952).
- [10] H. Saito, Y. Matsui, and M. Sakaki, "Discharge properties in low vacuum and vacuum monitoring method for vacuum circuit breakers," in *Proc. ISDEIV*, 2006, pp. 181–184, doi: [10.1109/DEIV.2006.357262](https://doi.org/10.1109/DEIV.2006.357262).
- [11] M. Kamarol, S. Ohtsuka, M. Hikita, H. Saitou, and M. Sakaki, "Determination of gas pressure in vacuum interrupter based on partial discharge," *IEEE Trans. Dielectr. Electr. Insul.*, vol. 14, no. 3, pp. 593–599, Jun. 2007, doi: [10.1109/TDEL.2007.369518](https://doi.org/10.1109/TDEL.2007.369518).
- [12] G.-Y. Lee, G.-S. Kil, and S.-W. Kim, "Partial discharge characteristics for internal defects of vacuum interrupters," *J. Korean Soc. Railway*, vol. 24, no. 3, pp. 274–279, Mar. 2021.
- [13] J. K. Sung, C. B. Park, G. H. Choi, J. H. You, and H. W. Hong, "A study on determination of live line for the distribution switchgear depending on VI's vacuum level," in *Proc. KIEE*, 2021, pp. 210–211.
- [14] S. Bang, H.-W. Lee, and B.-W. Lee, "Real-time monitoring of the vacuum degree based on the partial discharge and an insulation supplement design for a distribution class vacuum interrupter," *Energies*, vol. 14, no. 23, p. 7891, Nov. 2021, doi: [10.3390/en14237891](https://doi.org/10.3390/en14237891).
- [15] Z. Xin, L. Xu-Doing, F. Xing-Ming, H. Zhi-Chao, F. Jian-Rong, L. Cong, and S. Wei-Jian, "A high accurate sensor research and its application for VCBs' internal pressure on-line condition monitor," in *Proc. ISDEIV*, Sep. 2012, pp. 477–480, doi: [10.1109/DEIV.2012.6412559](https://doi.org/10.1109/DEIV.2012.6412559).
- [16] H. W. Lee, S. Bang, and B. W. Lee, "Study on vacuum degree prediction technology of vacuum interrupter through AC/DC partial discharge measurement," in *Proc. KIEE*, 2021, pp. 12–13.
- [17] *High-Voltage Test Techniques-Partial Discharge Measurements*, Standard IEC 60270, 2000.
- [18] D.-H. Oh, H.-S. Kim, and B.-W. Lee, "A novel diagnosis method for void defects in HVDC mass-impregnated PPLP cable based on partial discharge measurement," *Energies*, vol. 14, no. 8, p. 2052, Apr. 2021, doi: [10.3390/en14082052](https://doi.org/10.3390/en14082052).



research interests include HVDC protection systems, high voltage insulation, renewable energies, and development of electrical equipment, including transmission line structures for HVDC and HVAC power systems.

**SEUNGMIN BANG** received the B.S. and M.S. degrees from the Department of Electrical Engineering, Korea National University of Transportation, Chungju-si, South Korea, in 2015 and 2017, respectively. He is currently pursuing the Ph.D. degree with the Department of Electronic Engineering, Hanyang University, Ansan, South Korea. He was an Assistant Research Engineer at ENTEC Electric & Electronic Company, Ltd., South Korea, from 2017 to 2020. His



HVDC protection systems, high voltage insulation, renewable energies, development of electrical equipment, and transmission line structures for HVDC and HVAC power systems. He is a member of HVDC Research Committee of KIEE, Power Cable Experts Committee of the Korean Agency for Technology and Standards, and CIGRE.

**BANG-WOOK LEE** (Senior Member, IEEE) received the B.S., M.S., and Ph.D. degrees from the Department of Electrical Engineering, Hanyang University, Seoul, South Korea, in 1991, 1993, and 1998, respectively. He was a Senior Research Engineer at LS Industrial Systems Company, Ltd., South Korea. In 2008, he joined the Department of Electronic Engineering, Hanyang University, Ansan, South Korea, where he is currently a Professor. His research interests include

...



**HYUN-WOO LEE** received the B.S. degree from the Department of Electronic System Engineering, Hanyang University, Seoul, South Korea, in 2020. He is currently pursuing the M.S degree with the Department of Electronic Engineering, Hanyang University, Ansan, South Korea. His research interests include HVDC protection systems, high voltage insulation, renewable energies, development of electrical equipment, and transmission line structures for HVDC and HVAC power systems.